

FUDMA Journal of Sciences (FJS) ISSN online: 2616-1370 ISSN print: 2645 - 2944 ol. 9 No. 11 November, 2025, pp.83 -9

Vol. 9 No. 11, November, 2025, pp 83 –97



DOI: https://doi.org/10.33003/fjs-2025-0911-4073

ACCURATE BLOCK HYBRID METHODS FOR LARGE SCALE CHEMICAL KINETICS SIMULATIONS OF THE HIGH IRRADIANCE (HIRES) PROBLEM

*1Richard Olatokunbo Akinola, 2Shangkum Yildum Goji, 1Kyaharnan Victor Joshua and 1Amin Miracle Daze

¹Department of Mathematics, Faculty of Natural Sciences, University of Jos, Nigeria. ²Department of Chemistry, Faculty of Natural Sciences, University of Jos, Nigeria.

Correspondent Author's E-mail: roakinola@gmail.com

ABSTRACT

This article presents two A(a), zero–stable, consistent and convergent methods for the numerical approximation of the High Irraddiance problem. The first method is a first derivative method while the second method is a second derivative block hybrid method for the numerical solution of initial problems most especially the High Irraddiance (HIRES) problem with origins from chemical kinetics. The first method is of order five with a small region of absolute stability, while the new second derivative method is of order nine with a large region of absolute stability as well as smaller error constants. The methods stems from the interpolation and collocation approach with un-equidistant give points. Sequel to using the methods in solving the HIRES problem which has no exact solution, we compared the performance of our second method with a method in a recent literature and the method outperformed it. This gave us the motivation in using the method to solve the problem under consideration.

Keywords: Hires Problem, Block Hybrid, Absolute Stability, Interpolation, Collocation, Exact Solution

INTRODUCTION

Large-scale chemical kinetics simulations are fundamental to understanding complex reactive systems in scientific and engineering domains such as combustion modeling (Zhang et al,. 2022; Lu & Law, 2009) atmospheric chemistry (Mashruk et al., 2024), nuclear fusion (Jacobson, 2005), and astrophysical processes (Simon et al., 2007). One particularly demanding area is the High Irradiance (HIRES) problem, which involves modeling chemical transformations in environments subjected to intense radiation fields, such as in high-power laser systems or solar plasma phenomena. These scenarios are characterized by extremely rapid reaction dynamics, highly stiff differential systems, and extensive reaction networks, often involving thousands of chemical species and reaction pathways (Trieschmann et al., 2023; Bennett et al., 2011). Conventional numerical methods-both explicit and implicit-encounter severe challenges when applied to the HIRES problem. Explicit solvers are restricted by the stiffness of the chemical kinetic equations, necessitating extremely small-time steps, while implicit methods, though stable, involve complex matrix operations that scale poorly with system size (Hawagfeh & Kaya, 2004; Abdullahi, 2018). To overcome these issues, researchers have proposed Block Hybrid Methods—a family of numerical integrators that blend the features of multistep and Runge-Kutta schemes, enabling enhanced accuracy and stability while maintaining computational tractability (Rufai, 2024; Singh et al., 2021). Block hybrid methods allow for the simultaneous computation of multiple solution points within a time step, improving parallelizability and offering flexibility in handling stiff reactions. These advantages become particularly useful in the HIRES context, computational intensity and accuracy must be tightly balanced. Recent innovations in computationally efficient block hybrid methods have incorporated techniques such as adaptive time-stepping (Spiteri, 1997), Jacobian sparsity exploitation, and high-performance linear algebra routines to reduce overhead and improve scalability on parallel computing architectures (Kowalski et al., 2021; Castro et al., 2024). In their pioneering work, Smith and Anderson (Smith & Anderson, 2005) addressed the computational difficulties

posed by high irradiance in photovoltaic cells by developing a first-order HIRES method. Their approach involved adjusting the step size of the numerical solution in response to the irradiance levels, thereby enhancing stability. This method represented a significant improvement over traditional Euler methods, particularly in scenarios where irradiance changes rapidly. They developed a first-order numerical method that adapts to high irradiance conditions, ensuring both stability and accuracy. However, their method is of first-order, but in this paper, we present two block methods for the numerical solution of the HIRES problem. Recently the problem was also solved using the variational method and the numerical solution of the HIRES problem at five minutes. At this time, six solutions were obtained and at three hundred and fifty minutes for the remaining two (Amat et al., 2019).

Amat et al (2019) presented the numerical solution of the HIRES problem for different concentrations at different time intervals. Stiff systems of ODEs face severe time step restrictions, especially for large simulation times. The new variational method proposed by Amat et al (2019) has been successfully applied to stiff ODEs arising from chemical reactions with large systems. The variational method has the advantage of never getting stuck at local minima and always converges to the solution regardless of the initialization, unlike implicit Runge-Kutta methods. Nevertheless, the solutions they gave was not compared with any other methods in the literature. Here, we compared our solution to the HIRES problem with the well known stiff ODE solver ode15s for different step sizes; and our results are promising. This study explores the development and application of computationally efficient two block hybrid methods for simulating large-scale chemical kinetics under high irradiance conditions. By tailoring these advanced numerical schemes to the unique demands of the HIRES problem, this work aims to establish a reliable and scalable framework capable of handling the mathematical and computational complexities inherent in such simulations.

MATERIALS AND METHODS

A k-step first and second derivative block hybrid linear multistep methods for the numerical solution of ordinary differential equation are respectively (Lambert, 1973):

$$y(x) = \sum_{j=0}^{k} \alpha_j \, y_{n+j} + h \sum_{j=0}^{k} \beta_j \, f_{n+j}, \tag{1}$$

$$y(x) = \sum_{j=0}^{k} \alpha_j \, y_{n+j} + h \sum_{j=0}^{k} \beta_j \, f_{n+j} + h^2 \sum_{j=0}^{k} \gamma_j \, g_{n+j},$$
(2)

where the α_i , β_i and γ_i 's are unknown polynomials, $y_{n+j} = y(x_n + jh)$, is an approximate solution $y'(x_{n+j}) = f_{n+j} = f(x_n + jh, y(x_n + jh)),$

$$y''(x_{n+j}) = f'_{n+j} = f'(x_n + jh, y(x_n + jh)) = g_{n+j}.$$

Besides, the continuous coefficients are

$$\alpha_j(x) = \sum_{j=0}^k \alpha_{j,j+1} x^j, \beta_j(x) = \sum_{j=0}^k \beta_{j,j+1} x^j,$$

$$\gamma_j(x) = \sum_{j=0}^k \gamma_{j,j+1} x^j, \text{for } j = 0 (1) \dots, k-1.$$

The following matrix equation PQ = I, is solved where $I \in$ $R^{(t+m)\times(t+m)}$ is an identity matrix, P and Q are real $(t+m) \times (t+m)$ matrices (t interpolation points $0 < t \le$ k) and m collocation points, to obtain $\alpha_i(x)$, $\beta_i(x)$ and $\gamma_i(x)$ which are the first rows of Q (Onumanyi et al., 1994).

Derivation of the New First Derivative Hybrid Block Linear Multistep Method (FDHBLMM)

Let $y_n = y(x_n)$ and $f_n = f(x_n, y_n), y_{n+i} = y(x_{n+i}) = y(x_n + ih),$ for $x_i = x_0 + ih, i \in \{1, \frac{4}{3}, \frac{9}{5}, 2\},$ $h = \frac{b-a}{4}, f_{n+i} = \frac{b-a}{4}, f_{n+i}$ $f(x_{n+i},y_{n+i}) = f(x_n + ih,y(x_n + ih))$. By making the substitution t = 1, m = 5 and the above into equation (1), we obtained the continuous formulation:

$$y(x) = \alpha_0(x)y_n + h\left[\beta_0(x)f_n + \beta_1(x)f_{n+1} + \beta_{\frac{4}{3}}(x)f_{n+\frac{4}{3}} + \beta_{\frac{9}{5}}(x)f_{n+\frac{9}{5}} + \beta_2(x)f_{n+2}\right]. \tag{3}$$

The matrix *P* becomes:

$$P = \begin{bmatrix} 1 & x_n & x_n^2 & x_n^3 & x_n^4 & x_n^5 \\ 0 & 1 & 2x_n & 3x_n^2 & 4x_n^3 & 5x_n^4 \\ 0 & 1 & 2x_{n+1} & 3x_{n+1}^2 & 4x_{n+1}^3 & 5x_{n+1}^4 \\ 0 & 1 & 2x_{n+\frac{4}{3}} & 3x_{n+\frac{4}{3}}^2 & 4x_{n+\frac{4}{3}}^3 & 5x_{n+\frac{4}{3}}^4 \\ 0 & 1 & 2x_{n+\frac{9}{5}} & 3x_{n+\frac{9}{5}}^2 & 4x_{n+\frac{9}{5}}^3 & 5x_{n+\frac{9}{5}}^4 \\ 0 & 1 & 2x_{n+2} & 3x_{n+2}^2 & 4x_{n+2}^3 & 5x_{n+\frac{9}{5}}^4 \end{bmatrix}.$$

$$(4)$$

By replacing x_n with $x_{n+1} - h$, $x_{n+\frac{4}{3}} = x_{n+1} + \frac{h}{3}$, $x_{n+\frac{9}{2}} = x_{n+1} + \frac{4h}{5}$, $x_{n+2} = x_{n+1} + h$, the P matrix reduces to:

$$P = \begin{bmatrix} 1 & x_{n+1} - h & (x_{n+1} - h)^2 & (x_{n+1} - h)^3 & (x_{n+1} - h)^4 & (x_{n+1} - h)^5 \\ 0 & 1 & 2(x_{n+1} - h) & 3(x_{n+1} - h)^2 & 4(x_{n+1} - h)^3 & 5(x_{n+1} - h)^4 \\ 0 & 1 & 2x_{n+1} & 3x_{n+1}^2 & 4x_{n+1}^3 & 5x_{n+1}^4 \\ 0 & 1 & 2(x_{n+1} + \frac{1}{3}h) & 3(x_{n+1} + \frac{1}{3}h)^2 & 4(x_{n+1} + \frac{1}{3}h)^3 & 5(x_{n+1} + \frac{1}{3}h)^4 \\ 0 & 1 & 2(x_{n+1} + \frac{4}{5}h) & 3(x_{n+1} + \frac{4}{5}h)^2 & 4(x_{n+1} + \frac{4}{5}h)^3 & 5(x_{n+1} + \frac{4}{5}h)^4 \\ 0 & 1 & 2(x_{n+1} + h) & 3(x_{n+1} + h)^2 & 4(x_{n+1} + h)^3 & 5(x_{n+1} + h)^4 \end{bmatrix}.$$
 The determinant of the matrix above is $\frac{3584}{375}h^{10}$. The determinant of P is non–zero if and only if $\frac{3584}{375}h^{10}$ is non–zero or $h \neq 0$.

Now, we invert P using PQ = I where I is an identity matrix of size six by six. The first row of Q gives the continuous coefficients;

$$\alpha_0 = 1 \tag{6}$$

$$\beta_0(\psi) = -\frac{3\psi^5 + 8h\psi^4 + 7h^2\psi^3 + 2h^3\psi^2 - 20h^3}{72h^4} \tag{7}$$

$$\beta_1(\psi) = \frac{36\psi^3 + 51h\psi^4 - 44h^2\psi^3 - 102h^3\psi^2 - 48h^4\psi + 107h^3}{48h^4}$$
(8)

$$\beta_{\frac{4}{3}}(\psi) = -\frac{81\psi^5 + 81h\psi^4 - 135h^2\psi^3 - 162h^3\psi^2 + 135h^5}{56h^4}$$
(9)

$$\beta_{\frac{9}{5}}(\psi) = \frac{1500\psi^5 + 625h\psi^4 - 2500h^2\psi^3 - 1250h^3\psi^2 + 1625h^5}{1008h^4}$$
(10)

$$\beta_2(\psi) = -\frac{18\psi^5 + 3h\psi^4 - 26h^2\psi^3 - 12h^3\psi^2 + 17h^5}{24h^4}.$$
 (11)

Plugging the above into (3), the continuous formulation below is immediate

$$y(x) = y_n - \frac{(3\psi^5 + 8h\psi^4 + 7h^2\psi^3 + 2h^3\psi^2 - 20h^5)}{72h^4} f_n$$

$$+ \frac{(36\psi^5 + 51h\psi^4 - 44h^2\psi^3 - 102h^3\psi^2 - 48h^4\psi + 107h^5)48h^4}{f} - \frac{(81\psi^5 + 81h\psi^4 - 135h^2\psi^3 - 162h^3\psi^2 + 135h^5)56h^4}{f} - \frac{(1500\psi^5 + 625h\psi^4 - 2500h^2\psi^3 - 1250h^3\psi^2 + 1625h^5)}{1008h^4} f_{n+\frac{9}{5}}$$

$$- \frac{(18\psi^5 + 3h\psi^4 - 26h^2\psi^3 - 12h^3\psi^2 + 17h^5)}{24h^4} f_{n+2}.$$

We evaluated the continuous formulation above at $\psi=0$, $\psi=-\frac{h}{2}$, $\psi=-\frac{7}{9}$ and $\psi=-h$ using $x=x_{n+1}-\psi$. When $\psi=0$, $x=x_{n+1}$, $y(x)=y_{n+1}$; if $\psi=-\frac{h}{2}$, then $x=x_{n+\frac{3}{2}}$. Hence, $y(x)=y_{n+\frac{3}{2}}$. If $\psi=-\frac{7h}{9}$, then $x=x_{n+\frac{16}{9}}$ and for $\psi=-h$, $x=x_{n+2}$. Hence, $y(x)=y_{n+2}$. The four discrete schemes below are immediate

$$y_{n+1} = y_n + \left[\frac{5}{18} f_n + \frac{107}{48} f_{n+1} - \frac{135}{56} f_{n+\frac{4}{3}} + \frac{1625}{1008} f_{n+\frac{9}{5}} - \frac{17}{24} f_{n+2} \right] h \tag{12}$$

$$y_{n+\frac{4}{3}} = y_n + \left[\frac{202}{729} f_n + \frac{64}{27} f_{n+1} - \frac{46}{21} f_{n+\frac{4}{3}} + \frac{8000}{5103} f_{n+\frac{9}{5}} - \frac{56}{81} f_{n+2} \right] h \tag{13}$$

$$y_{n+\frac{9}{5}} = y_n + \left[\frac{1737}{6250} f_n + \frac{116397}{50000} f_{n+1} - \frac{334611}{175000} f_{n+\frac{4}{3}} + \frac{5193}{2800} f_{n+\frac{9}{5}} - \frac{18711}{25000} f_{n+2} \right] h \tag{14}$$

$$y_{n+2} = y_n + \left[\frac{5f_n}{18} f_n + \frac{7}{3} f_{n+1} - \frac{27}{14} f_{n+\frac{4}{3}} + \frac{125}{63} f_{n+\frac{9}{5}} - \frac{2}{3} f_{n+2} \right] h. \tag{15}$$

The new Ninth Order Second Derivative Block Hybrid Linear Multistep Method (NOSDBHLMM)

For our derivation, we used one interpolation point and ten collocation points to derive the continuous formulation of the new second derivative method:

$$y(x) = \alpha_0(x)y_n + h\left[\beta_0(x)f_n + \beta_1(x)f_{n+1} + \beta_{\frac{4}{3}}(x)f_{n+\frac{4}{3}} + \beta_{\frac{9}{5}}(x)f_{n+\frac{9}{5}} + \beta_2(x)f_{n+2}\right] + h^2\left[\gamma_0(x)g_n + \gamma_1(x)g_{n+1} + \gamma_{\frac{4}{3}}(x)g_{n+\frac{4}{3}} + \gamma_{\frac{9}{5}}(x)g_{n+\frac{9}{5}} + \gamma_2(x)g_{n+2}\right].$$
(16)

Thus, the matrix D becomes

$$D_{1} = \begin{bmatrix} 1 & x_{n} & x_{n}^{2} & x_{n}^{3} & x_{n}^{4} & x_{n}^{5} & x_{n}^{6} & x_{n}^{7} & x_{n}^{8} & x_{n}^{9} & x_{n}^{10} \\ 0 & 1 & 2x_{n} & 3x_{n}^{2} & 4x_{n}^{3} & 5x_{n}^{4} & 6x_{n}^{5} & 7x_{n}^{6} & 8x_{n}^{7} & 9x_{n}^{8} & 10x_{n}^{9} \\ 0 & 1 & 2x_{n+1} & 3x_{n+1}^{2} & 4x_{n+1}^{3} & 5x_{n+1}^{4} & 6x_{n+1}^{5} & 7x_{n+1}^{6} & 8x_{n+1}^{7} & 9x_{n+1}^{8} & 10x_{n+1}^{9} \\ 0 & 1 & 2x_{n+\frac{4}{3}} & 3x_{n+\frac{4}{3}}^{2} & 4x_{n+\frac{4}{3}}^{3} & 5x_{n+\frac{4}{3}}^{4} & 6x_{n+\frac{4}{3}}^{5} & 7x_{n+\frac{4}{3}}^{6} & 8x_{n+\frac{4}{3}}^{7} & 9x_{n+\frac{4}{3}}^{8} & 10x_{n+\frac{4}{3}}^{9} \\ 0 & 1 & 2x_{n+\frac{9}{5}} & 3x_{n+\frac{9}{5}}^{2} & 4x_{n+\frac{9}{5}}^{3} & 5x_{n+\frac{9}{5}}^{4} & 6x_{n+\frac{9}{3}}^{5} & 7x_{n+\frac{4}{3}}^{6} & 8x_{n+\frac{9}{3}}^{7} & 9x_{n+\frac{9}{5}}^{8} & 10x_{n+\frac{4}{3}}^{9} \\ 0 & 1 & 2x_{n+\frac{9}{5}} & 3x_{n+\frac{9}{5}}^{2} & 4x_{n+2}^{3} & 5x_{n+\frac{9}{5}}^{4} & 6x_{n+\frac{9}{5}}^{5} & 7x_{n+\frac{9}{5}}^{6} & 8x_{n+\frac{9}{2}}^{7} & 9x_{n+\frac{9}{5}}^{8} & 10x_{n+\frac{9}{3}}^{9} \\ 0 & 1 & 2x_{n+2} & 3x_{n+2}^{2} & 4x_{n+2}^{3} & 5x_{n+\frac{9}{5}}^{4} & 6x_{n+2}^{5} & 7x_{n+2}^{6} & 8x_{n+2}^{7} & 9x_{n+\frac{9}{5}}^{8} & 10x_{n+\frac{9}{3}}^{9} \\ 0 & 0 & 2 & 6x_{n} & 12x_{n}^{2} & 20x_{n}^{3} & 30x_{n}^{4} & 42x_{n}^{5} & 56x_{n}^{6} & 72x_{n}^{7} & 90x_{n+1}^{8} \\ 0 & 0 & 2 & 6x_{n+1} & 12x_{n+1}^{2} & 20x_{n+\frac{1}{3}}^{3} & 30x_{n+\frac{4}{3}}^{4} & 42x_{n+\frac{1}{3}}^{5} & 56x_{n+\frac{1}{3}}^{6} & 72x_{n+\frac{1}{3}}^{7} & 90x_{n+\frac{1}{3}}^{8} \\ 0 & 0 & 2 & 6x_{n+\frac{1}{3}} & 12x_{n+\frac{9}{3}}^{2} & 20x_{n+\frac{1}{3}}^{3} & 30x_{n+\frac{1}{3}}^{4} & 42x_{n+\frac{1}{3}}^{5} & 56x_{n+\frac{1}{3}}^{6} & 72x_{n+\frac{1}{3}}^{7} & 90x_{n+\frac{1}{3}}^{8} \\ 0 & 0 & 2 & 6x_{n+\frac{1}{3}} & 12x_{n+\frac{9}{3}}^{2} & 20x_{n+\frac{1}{3}}^{3} & 30x_{n+\frac{1}{3}}^{4} & 42x_{n+\frac{1}{3}}^{5} & 56x_{n+\frac{1}{3}}^{6} & 72x_{n+\frac{1}{3}}^{7} & 90x_{n+\frac{1}{3}}^{8} \\ 0 & 0 & 2 & 6x_{n+2} & 12x_{n+2}^{2} & 20x_{n+\frac{1}{3}}^{3} & 30x_{n+\frac{1}{3}}^{4} & 42x_{n+\frac{1}{3}}^{5} & 56x_{n+\frac{1}{3}}^{6} & 72x_{n+\frac{1}{3}}^{7} & 90x_{n+\frac{1}{3}}^{8} \\ 0 & 0 & 2 & 6x_{n+2} & 12x_{n+2}^{2} & 20x_{n+\frac{1}{3}}^{3} & 30x_{n+\frac{1}{3}}^{4} & 42x_{$$

We made the same substitutions into the D_1 matrix as those used in the derivation of the first derivative method above. After inverting the D_1 matrix premised on its non-singularity we obtained the first row of the C_1 matrix from $D_1C_1 = I$ which are: $\alpha_0 = 1$,

$$\begin{split} \beta_0(\varphi) &= \frac{h^+\phi^+ - 3188125000h^+\phi^+ 12813281250h^+\phi^+ - 2877000000h^+\phi^+ + 9001562500}{134452672h^+} + 1523500000h^+\phi^+ 15631862500\phi^{\pm 0} \\ &= \frac{h^+\phi^+ - 3188750000h^+\phi^+ - 195156250h^+\phi^+ - 1522500000h^+\phi^+ - 2843750h^+\phi^+ \\ -240000000h^+\phi^+ - 100078125h^+\phi^+ + 90250000h\phi^+ + 59062500\phi^{\pm 0} \\ &= \frac{-3006153h^+ + 1632960h^+\phi^+ - 4673560h^+\phi^+ + 641966h^+\phi^- - 5154030h^+\phi^+ \\ -11984760h^+\phi^- - 2372895h^+\phi^+ + 4932900h\phi^+ + 2296350\phi^+ \\ &= \frac{-10888455h^+ + 1469640h^+\phi^- + 2976606h^+\phi^+ + 551124h^+\phi^- - 37384578h^+\phi^- \\ -19683000h^+\phi^- + 1135823h^+\phi^+ + 1013940h^+\phi^+ + 1377810\phi^+ \\ &= \frac{-10888455h^+ + 1469640h^+\phi^- + 2976606h^+\phi^+ + 551124h^+\phi^- - 37384578h^+\phi^- \\ -19683000h^+\phi^- + 1135823h^+\phi^+ + 1013940h^+\phi^+ + 1377810\phi^+ \\ &= \frac{-1085845h^+\phi^- + 35354h^+\phi^+ + 255360h\phi^+\phi^+ + 1103800h^+\phi^- + 1473466h^+\phi^+ \\ &= \frac{-103569h^{10} - 53376h^+\phi^- + 87248h^+\phi^+ + 269186h^+\phi^+ + 174720h^+\phi^- - 225148h^+\phi^+ \\ &= \frac{-103569h^{10} - 5376h^+\phi^+ + 378820h^+\phi^+ + 133440h\phi^+ + 6420\phi^{\pm 0}}{33576h^+\phi^+ + 3080h^+\phi^+ + 74700h\phi^+ + 18900\phi^+ \\ &= \frac{-106080h^+\phi^- - 34055h^+\phi^+ + 313440h\phi^+ + 6420\phi^{\pm 0}}{13440h^+} \\ &= \frac{-106080h^+\phi^- - 241525h^+\phi^+ + 31826h^+\phi^- - 3358h^+\phi^+ + 29884h^+\phi^- - 20769h^+\phi^+ + 22330h\phi^+ + 15120\phi^{\pm 0}}{13440h^+} \\ &= \frac{-10561h^{10} - 3809h^+\phi^- + 21588h^+\phi^+ - 3350h^+\phi^- + 3390h^+\phi^- - 1715h^+\phi^+ + 13300h\phi^+ + 15120\phi^{\pm 0}}{13440h^+} \\ &= \frac{47541h^{10} - 2240h^+\phi^+ + 12500h^+\phi^+ + 21588h^+\phi^- - 3380h^+\phi^- - 1715h^+\phi^+ + 13300h\phi^+ + 9450\phi^{\pm 0}}{13240h^+\phi^+ + 325120h^+\phi^+ + 27600\phi^+\phi^+ + 21588h^+\phi^- - 1348500h^+\phi^- - 118390h^+\phi^- + 3876h^+\phi^- - 3376h^+\phi^- - 3376h^+\phi^- - 3480h^+\phi^- - 1715h^+\phi^+ + 3900h^+\phi^+ + 376h^+\phi^- - 1878500h^+\phi^+ + 14720h^+\phi^+ + 24760\phi^+ + 376h^+\phi^- - 387850h^+\phi^- - 3180h^+\phi^- - 1715h^+\phi^+ + 3900h^+\phi^+ + 15120\phi^+ + 3900h^+\phi^- + 247900000h^+\phi^+ + 2877000000h^+\phi^+ + 2877000000h^+\phi^+ + 2877000000h^+\phi^- - 28785h^+\phi^- - 38786h^+\phi^- - 198850h^+\phi^- + 191018400h^+\phi^- + 19118400h^+\phi^- + 191186h^+\phi^- +$$

We evaluated the continuous scheme at $\varphi = 0$, $\varphi = -h$, $\varphi = \frac{-h}{3}$, $\varphi = \frac{-4h}{5}$. Hence, we got the four discrete schemes which is what makes up the block method below

$$y_{n+1} = y_n + \left[\frac{729367}{2612736} f_n - \frac{34523}{1792} f_{n+1} + \frac{10858455}{1229312} f_{n+\frac{4}{3}} - \frac{3038046875}{448084224} f_{n+\frac{9}{5}} + \frac{4017}{224} f_{n+2} \right] h$$

$$\begin{split} &+\left[\frac{15847}{725760}g_{n}-\frac{39289}{13440}g_{n+1}+\frac{3006153}{439040}g_{n+\frac{4}{3}}-\frac{17234375}{3556224}g_{n+\frac{9}{5}}-\frac{7253}{6720}g_{n+2}\right]h^{2}\\ &y_{n+\frac{4}{3}}=y_{n}+\left[\frac{84121834}{301327047}f_{n}-\frac{7904576}{413343}f_{n+1}+\frac{21638}{2401}f_{n+\frac{4}{3}}-\frac{70100500000}{103355177121}f_{n+\frac{9}{5}}+\frac{7418720}{413343}f_{n+2}\right]h\\ &+\left[\frac{3655604}{167403915}g_{n}-\frac{6028672}{2066715}g_{n+1}+\frac{953684}{138915}g_{n+\frac{4}{3}}-\frac{7958000000}{1640558367}g_{n+\frac{9}{5}}-\frac{2232448}{2066715}g_{n+2}\right]h^{2}\\ &y_{n+\frac{9}{5}}=y_{n}+\left[\frac{1954322379}{7000000000}f_{n}-\frac{66838685031}{3500000000}f_{n+1}+\frac{22139918684883}{24010000000000}f_{n+\frac{4}{3}}-\frac{101657691}{15366400}f_{n+\frac{9}{5}}+\frac{7880266197}{437500000}f_{n+2}\right]h+\left[\frac{76439511}{3500000000}g_{n}-\frac{5100278643}{1750000000}g_{n+1}-\frac{1172635726761}{171500000000}g_{n+\frac{4}{3}}-\frac{26783163}{5488000}g_{n+\frac{9}{5}}-\frac{948189159}{6728750000000}g_{n+2}\right]h^{2}\\ &y_{n+2}=y_{n}+\left[\frac{34193}{122472}f_{n}-\frac{401}{21}f_{n+1}+\frac{177147}{19208}f_{n+\frac{4}{3}}-\frac{34140625}{5250987}f_{n+\frac{9}{5}}+\frac{380}{21}f_{n+2}\right]h\\ &+\left[\frac{743}{34020}g_{n}-\frac{102}{35}g_{n+1}-\frac{46899}{6860}g_{n+\frac{4}{3}}-\frac{406250}{83349}g_{n+\frac{9}{5}}-\frac{38}{35}g_{n+2}\right]h^{2}. \end{split}$$

Convergence Analysis for the First Derivative Block Hybrid Method

In this section, we examine the order, error constant, zero stability and convergence of the discrete schemes

Order and Error Constant of the First Derivative Block Hybrid Method

We summarize the order and error constant of the schemes derived above. We plotted the regions of absolute stability of the first derivative method.

A linear difference operator L associated with a linear multi-step method [23],

$$\sum_{j=0}^{k} \alpha_j(x) y_{n+j} = h \sum_{j=0}^{k} \beta_j(x) f_{n+j}, \text{for } j = 0, 1, \dots, k,$$
 such that $\alpha_0^2 + \beta_0^2 > 0$ is given by

$$L[y(x);h] = \sum_{j=0}^{k} \left[\alpha_j y(x+jh) - h \beta_j y'(x+jh) \right]$$

= $C_0 y(x) + C_1 h y^{(1)}(x) + \dots + C_p h^p y^{(p)}(x) + \dots$, (19)

 C_{y} 's are real and y(x) is any arbitrary function which is continuously differentiable on an interval.

Definition 2.1. A linear multistep method and the associated difference operator (19) is of order p if, $C_0 = C_1 = \cdots = C_p = C_{p+1} \neq 0$, where C_{p+1} is the error constant of the method.

Furthermore,

$$\begin{split} C_0 &= \sum_{i=0}^k \alpha_i, \\ C_1 &= \sum_{i=1}^k (i\alpha_i - \beta_i), \\ C_2 &= \sum_{i=1}^k \left(\frac{i^2}{2}\alpha_i - i\beta_i\right), \\ \vdots \\ C_p &= \sum_{i=1}^k \left(\frac{i^p\alpha_i}{p!} - \frac{i^{p-1}\beta_l}{(p-1)!}\right), \end{split}$$

for $p \ge 2$. The unknown vectors from (12)–(15) are

$$\alpha_{0} = -\begin{bmatrix} 1\\1\\1\\1 \end{bmatrix}, \alpha_{1} = \begin{bmatrix} 1\\0\\0\\0 \end{bmatrix}, \alpha_{\frac{4}{3}} = \begin{bmatrix} 0\\1\\0\\0 \end{bmatrix}, \alpha_{\frac{9}{5}} = \begin{bmatrix} 0\\0\\1\\0 \end{bmatrix}, \alpha_{2} = \begin{bmatrix} 0\\0\\0\\1 \end{bmatrix}, \alpha_{2} = \begin{bmatrix} 0\\0\\0\\1 \end{bmatrix}, \alpha_{2} = \begin{bmatrix} 0\\0\\0\\1 \end{bmatrix}, \alpha_{3} = \begin{bmatrix} 0\\0\\0\\1 \end{bmatrix}, \alpha_{4} = \begin{bmatrix} 0\\0\\0\\1 \end{bmatrix}, \alpha_{5} = \begin{bmatrix} \frac{5}{18}\\\frac{202}{729}\\\frac{7737}{6250}\\\frac{5}{18} \end{bmatrix}, \beta_{1} = \begin{bmatrix} \frac{107}{48}\\\frac{64}{27}\\\frac{116397}{50000}\\\frac{7}{3} \end{bmatrix}, \beta_{\frac{4}{3}} = \begin{bmatrix} -\frac{135}{56}\\-\frac{46}{21}\\-\frac{334611}{175000}\\-\frac{27}{14} \end{bmatrix}, \beta_{\frac{9}{5}} = \begin{bmatrix} \frac{1625}{1008}\\\frac{8000}{5103}\\\frac{5193}{2800}\\\frac{125}{63} \end{bmatrix}, \beta_{2} = \begin{bmatrix} -\frac{17}{24}\\-\frac{56}{81}\\\frac{18711}{25000}\\-\frac{2}{3} \end{bmatrix}$$

The above formula implies: $C_i = 0$ for i = 0,1,2,3,4,5. Since C_6 is not equal to zero, the computed error constant are as shown in Table 1 and the order.

Table 1: The error constants and order of the discrete schemes that comprise the first derivative method

y _i	Order	Error Constatnt
y_{n+1}	5	$2.509259259259 \times 10^{-3}$
$y_{n+\frac{4}{3}}$	5	$2.477671086724585 \times 10^{-3}$
y _{n+} 9	5	$2.5293600000000000 \times 10^{-3}$
У _{n+2}	5	$2.518518518518519 \times 10^{-3}$

The Local Truncation Error (LTE) of order p can be expressed in the form

$$T_{n+k} = C_{p+1}h^{p+1}y^{(p+1)}(x_n) + O(h^{p+2}),$$

and the principal local truncation error is $C_{p+1}h^{p+1}y^{(p+1)}(x_n)$. Therefore, the LTE is

$$T_{n+2} = [2.5093, 2.4777, 2.5294, 2.5185]^T \times 10^{-3} h^6 y^{(6)}(x_n) + \mathcal{O}(h^7).$$

Order and Error Constant of the Second Derivative Block Hybrid Method

Examining the order, error constant, zero stability and convergence of the discrete schemes.

$$\mathcal{L}[y(x);h] = \sum_{j=0}^{k} \left[\alpha_{j} y(x+jh) - h\beta_{j} y'(x+jh) - h^{2} \gamma_{j} y''(x+jh) \right]$$

$$= C_{0} y(x) + C_{1} h y^{(1)}(x) + \dots + C_{p} h^{p} y^{(p)}(x) + \dots ,$$
(20)

A linear difference operator L associated with a linear multi-step method,

$$\sum_{j=0}^{k} \alpha_{j}(x) y_{n+j} = h \sum_{j=0}^{k} \beta_{j}(x) f_{n+j} + h^{2} \sum_{j=0}^{k} \gamma_{j}(x) g_{n+j}, \text{for } j = 0, 1, \dots, k,$$

is given by

 $C_p \in \mathbb{R}^n$ and y(x) is any arbitrary function that is twice continuously differentiable on an interval.

A linear multi-step method and the associated difference operator (20) is of order p if, $C_0 = C_1 = \cdots = C_p = C_{p+1} = 0$, $C_{p+2} \neq 0$, where C_{p+2} is the error constant of the second derivative block method.

The following vectors were obtained from (18)

$$\alpha_0 = -\begin{bmatrix} 1 \\ 1 \\ 1 \\ 1 \end{bmatrix}, \alpha_1 = \begin{bmatrix} 1 \\ 0 \\ 0 \\ 0 \end{bmatrix}, \alpha_{\frac{4}{3}} = \begin{bmatrix} 0 \\ 1 \\ 0 \\ 0 \end{bmatrix}, \alpha_{\frac{9}{5}} = \begin{bmatrix} 0 \\ 0 \\ 1 \\ 0 \end{bmatrix}, \alpha_2 = \begin{bmatrix} 0 \\ 0 \\ 0 \\ 1 \end{bmatrix}$$

$$\beta_0 = \begin{bmatrix} \frac{729367}{2612736} \\ \frac{84121834}{301327047} \\ \frac{1954322379}{7000000000} \\ \frac{34193}{122472} \end{bmatrix}, \beta_1 = -\begin{bmatrix} \frac{34523}{1792} \\ \frac{7904576}{413343} \\ \frac{66838685031}{3500000000} \\ \frac{401}{21} \end{bmatrix}, \beta_{\frac{4}{3}} = \begin{bmatrix} \frac{10858455}{1229312} \\ \frac{21638}{2401} \\ \frac{22139918684883}{24010000000000} \\ \frac{1777147}{19208} \end{bmatrix}, \beta_{\frac{9}{5}} = -\begin{bmatrix} \frac{3038046875}{448084224} \\ \frac{701005000000}{100355177121} \\ \frac{101657691}{15366400} \\ \frac{34140625}{5250987} \end{bmatrix}$$

$$\beta_2 = \begin{bmatrix} \frac{4017}{224} \\ \frac{7418720}{473343} \\ \frac{7880266197}{437500000} \\ \frac{380}{21} \end{bmatrix}, \gamma_0 = \begin{bmatrix} \frac{15847}{725760} \\ \frac{3655604}{167403915} \\ \frac{76439511}{35000000000} \\ \frac{743}{34020} \end{bmatrix}, \gamma_1 = -\begin{bmatrix} \frac{39289}{13440} \\ \frac{6028672}{2066715} \\ \frac{5100278643}{1750000000} \\ \frac{102}{35} \end{bmatrix}, \gamma_{\frac{4}{3}} = -\begin{bmatrix} \frac{3006153}{489940} \\ \frac{953684}{138915} \\ \frac{1172635726761}{171500000000} \\ \frac{46899}{6860} \end{bmatrix}$$

$$\gamma_{\frac{9}{5}} = -\begin{bmatrix} \frac{17234375}{3556224} \\ \frac{7958000000}{1640558367} \\ \frac{26783163}{5488000} \\ \frac{406250}{83349} \end{bmatrix}, \gamma_{2} = -\begin{bmatrix} \frac{7253}{6720} \\ \frac{2232448}{2266715} \\ \frac{948189159}{875000000} \\ \frac{35}{38} \end{bmatrix}$$

We used the vectors above in:

$$\begin{split} C_0 &= \sum_{i=0}^k \alpha_i, \\ C_1 &= \sum_{i=1}^k i\alpha_i - \sum_{i=0}^k \beta_i, \\ C_2 &= \sum_{i=1}^k \left(\frac{i^2}{2}\alpha_i - i\beta_i\right), \\ \vdots \\ C_q &= \frac{1}{q!} \sum_{i=1}^k i^p \alpha_i - \frac{1}{(q-1)!} \sum_{i=1}^k i^{p-1} \beta_i - \frac{1}{(q-2)!} \sum_{i=1}^k i^{q-2} \gamma_i, \quad q \geq 3, \end{split}$$

and discovered that $C_0 = C_1 = C_2 = \cdots = C_9 = C_{10} = 0$ but $C_{11} = C_{p+2} \neq 0$. C_{p+2} is the error constant, at the point x_n , the principal truncation error is $C_{p+2}h^{p+2}y^{p+2}(x_n)$ and the local truncation error is $LTE = C_{p+2}h^{p+2}y^{p+2}(x_n) + O(h^{p+3})$.

The error constants C_{11} as well as the order are shown in Table 2.

Table 2: Table showing the error constants of the discrete schemes

y _i	Order	Error Constant $C_{11} \neq 0$
y_{n+1}	9	$3.474723014699499 \times 10^{-8}$
$y_{n+\frac{4}{3}}$	9	$3.476171358147117 \times 10^{-8}$
$y_{n+\frac{9}{5}}$	9	$3.478981758812616 \times 10^{-8}$
y _{n+1}	9	$3.479265090082256 \times 10^{-8}$

The LTE for the second derivative method is

$$LTE = [3.4747, 3.4762, 3.4790, 3.4793]^T \times 10^{-8}h^{11}y^{11}(x_n) + \mathcal{O}(h^{12}).$$

Region of Absolute Stability of the First Derivative Block Method

To plot the region of absolute stability of the first derivative method, we express the new method as:

$$\begin{bmatrix} 1 & 0 & 0 & 0 \\ 0 & 1 & 0 & 0 \\ 0 & 0 & 1 & 0 \\ 0 & 0 & 0 & 1 \end{bmatrix} \begin{bmatrix} y_{n+1} \\ y_{n+\frac{4}{3}} \\ y_{n+\frac{9}{5}} \\ y_{n+2} \end{bmatrix} = \begin{bmatrix} 0 & 0 & 0 & 1 \\ 0 & 0 & 0 & 1 \\ 0 & 0 & 0 & 1 \\ 0 & 0 & 0 & 1 \end{bmatrix} \begin{bmatrix} y_{n+1} \\ y_{n+2} \\ y_{n+3} \\ y_n \end{bmatrix}$$

$$\begin{aligned} & \text{and} A = I \in R^{4 \times 4} \\ B = \begin{bmatrix} 0 & 0 & 0 & 1 \\ 0 & 0 & 0 & 1 \\ 0 & 0 & 0 & 1 \\ 0 & 0 & 0 & 1 \end{bmatrix}, \\ K = \begin{bmatrix} \frac{107}{48} & -\frac{135}{56} & \frac{1625}{1008} & -\frac{17}{24} \\ \frac{64}{27} & -\frac{46}{21} & \frac{8000}{5103} & -\frac{56}{81} \\ \frac{116397}{5000} & -\frac{334611}{17500} & \frac{5193}{2800} & -\frac{18711}{25000} \\ \frac{7}{3} & -\frac{27}{14} & \frac{125}{63} & -\frac{2}{3} \end{bmatrix}, G = \begin{bmatrix} 0 & 0 & 0 & \frac{5}{18} \\ 0 & 0 & 0 & \frac{202}{729} \\ 0 & 0 & 0 & \frac{1737}{6250} \\ 0 & 0 & 0 & \frac{5}{18} \end{bmatrix}$$

We utilized the above matrices to find the zeros of the stability polynomial det[(wA - B - zG - zwK)],

where $y' = \lambda y$, $z = \lambda h$ is the usual test equation, $\mu = e^{i\theta}$, $0 \le \theta \le 2\pi$ and i is the imaginary unit of a complex number. This yields the stability polynomial:

$$\rho(\mu,z) = \frac{\left[(36\mu^4 - 2\mu^3)z^4 - (202\mu^4 - 32\mu^3)z^3 + (621\mu^4 - 213\mu^3)z^2 - (1104\mu^4 + 696\mu^3)z + 900\mu^4 - 900\mu^3 \right]}{900}$$

We plotted the region of absolute stability of the new first derivative method using the stability polynomial above and the graph is shown in Figure 1.

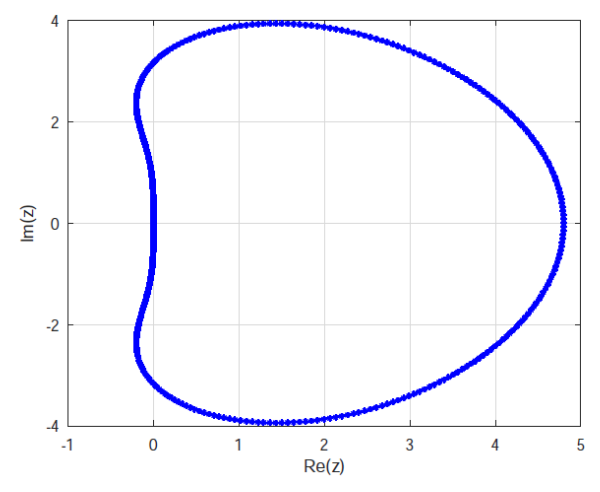
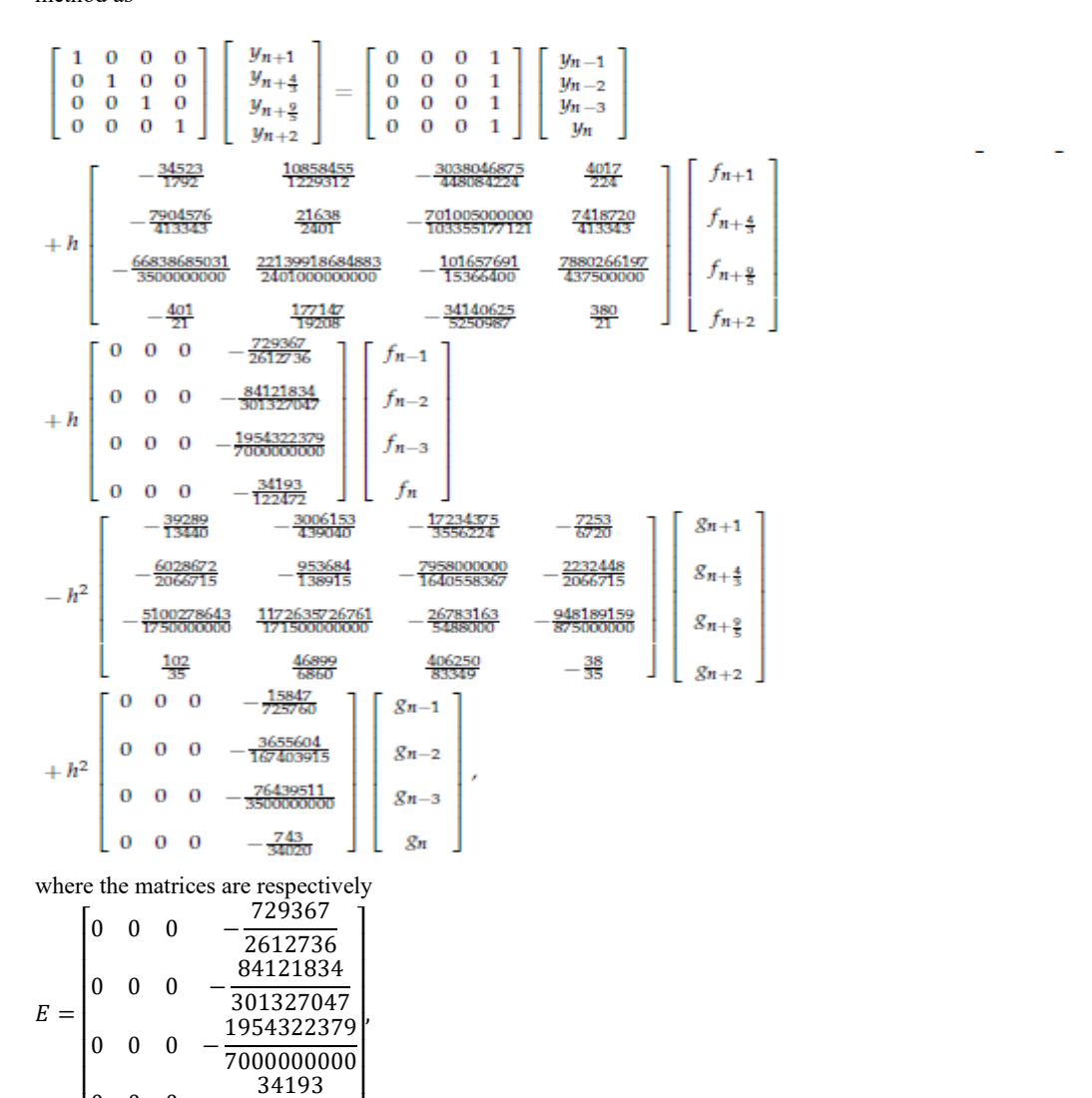


Figure 1: Region of absolute stability for the new method

Figure 1 shows the region of absolute stability of the first derivative block hybrid method which is $A(\alpha)$ -stable. The stability region is the interior of the contour on the left half plane of Figure 1.

Region of Absolute Stability of the Second Derivative Block Hybrid Method

Here, we want to plot the graph of the absolute stability of the method for the numerical solution of IVPs. Following (Okuonghae & Ikhile, 2012) and as used in (Akinola & Akoh, 2024), one can write the new second derivative block hybrid method as



122472

$$T = \begin{bmatrix} -\frac{34523}{1792} & \frac{10858455}{1229312} & -\frac{3038046875}{448084224} & \frac{4017}{224} \\ -\frac{7904576}{413343} & \frac{21638}{2401} & -\frac{70100500000}{103355177121} & \frac{413343}{413343} \\ -\frac{66838685031}{350000000} & \frac{22139918684883}{2401000000000} & -\frac{101657691}{15366400} & \frac{7880266197}{437500000} \\ -\frac{401}{21} & \frac{177147}{19208} & -\frac{34140625}{5250987} & \frac{380}{21} \end{bmatrix}$$

$$P = \begin{bmatrix} -\frac{39289}{13440} & -\frac{3006153}{439040} & -\frac{17234375}{3556224} & -\frac{7253}{6720} \\ -\frac{6028672}{2066715} & -\frac{953684}{138915} & -\frac{7958000000}{1640558367} & -\frac{7253}{6720} \\ -\frac{5100278643}{1750000000} & \frac{11726035726761}{171500000000} & -\frac{26783163}{83349} & -\frac{948189159}{35} \end{bmatrix}$$
and
$$M = \begin{bmatrix} 0 & 0 & 0 & -\frac{15847}{725760} \\ 0 & 0 & 0 & -\frac{3655604}{167403915} \\ 0 & 0 & 0 & -\frac{76439511}{3500000000} \\ 0 & 0 & 0 & -\frac{743}{34020} \end{bmatrix}$$

We substituted the above matrices into the characteristics equation

$$\det[r(A - Tz - Pz^{2}) - (B + Ez + Mz^{2})] = 0.$$

Here we have that $y' = \lambda y$, $y'' = \lambda^2 y$, $z = \lambda h$ and $z^2 = \lambda^2 h^2$ which are the typical test equations. The characteristic polynomial becomes

$$\rho(r,z) = \frac{((648r^4 - 2r^3)z^8 + (-(10908r^4) - 96r^3)z^7 + (105918r^4 - 2388r^3)z^6 + (-(726570r^4) - 37560r^3)z^5 + (3697965r^4 - 399285r^3)z^4}{51030000} \\ + \frac{(-(13906620r^4) - 2896740r^3)z^3 + (36978480r^4 - 13844880r^3)z^2}{+(-(62596800r^4) - 13844880r^3)z + 51030000r^4 - 51030000r^3)}{51030000}.$$

Differentiating $\rho(r, z)$ partially with respect to z;

$$\frac{\partial \rho(r,z)}{\partial z} = \frac{(8(648r^4 - 2r^3)z^7 + 7(-(10908r^4) - 96r^3)z^6 + 6(105918r^4 - 2388r^3)z^5}{+5(-(726570r^4) - 37560r^3)z^4 + 4(3697965r^4 - 399285r^3)z^3}{51030000}$$

$$\frac{3(-(13906620r^4) - 2896740r^3)z^2 + 2(36978480r^4)z^4}{+\frac{-13844880r^3)z + (-(62596800r^4) - 13844880r^3)}{51030000}.$$

We plotted the graph of the region of absolute stability making use of Newton's method for finding the roots of the above stability polynomial.

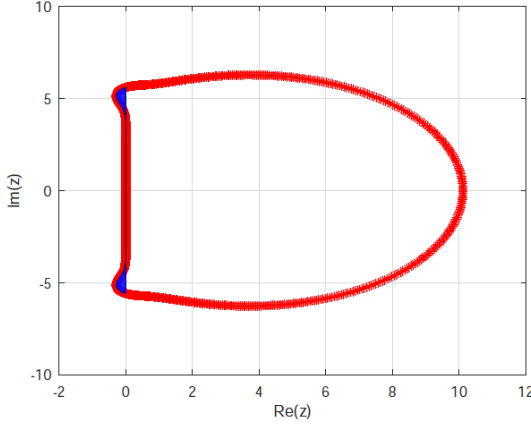


Figure 2: Region of absolute stability for the second derivative method

Figure 2 shows that the region of absolute stability of the stability polynomial above is $A(\alpha)$ –Stable. The stability region is the part of the contour shaded in blue. We state that though the two new methods are $A(\alpha)$ –stable, the second method has a larger region of absolute stability than the first method.

Zero Stability of the Two Block Hybrid Methods

Next, to ascertain the zero-stability of the two methods, we let z = 0 in

 $\det \Box rA - B - zG - zrK$

such that $\det(rA-B) = 0$. Since the roots of the above polynomial are zero and one of multiplicities three and one respectively, the first and second derivative methods are both zero stable by definition. Observe that since the order of the first and second derivative methods are five and nine respectively, they are both consistent. Besides, since both methods are consistent and zero-stable as shown above, the two new methods converges by definition (Yakubu & Sibanda, 2024).

Numerical Experiments

In this section, we compared the maximum absolute errors of the linear problem in (Henrici, 1962) which has an exact solution with those of the methods in this paper to see how accurate our solutions are; we found out that our methods performed better than (Henrici, 1962). This is what gave us the needed motivation to using it in solving the HIRES Problem. In comparing the results of our methods with those of Amat et al., (2019) on the HIRES problem, we used the solution provided by ode15s as the exact solution.

Example 1: Linear Problem

We consider the system [18]

$$p'(t) = -21p + 19q - 20r$$

$$q'(t) = 19p - 21q + 20r$$

$$r'(t) = 40p - 40q - 40r$$

on the interval [0,4] with [p(0),q(0),r(0)]=[1,0,-1] and exact solution

$$p(t) = 0.5[\exp(-2t) + \exp(-40t)(\cos(40t) + \sin(40t))]$$

$$q(t) = 0.5[\exp(-2t) - \exp(-40t)(\cos(40t) + \sin(40t))]$$

$$r(t) = \exp(-40t)[\sin(40t) - \cos(40t)].$$

Result of our computational simulation can be found in Table 3 with different step sizes and Figure 3 with a constant step size of $h = \frac{1}{160}$.

Table 3: Results of Example 1

Steps	h	Max Error	Max Error	Max Error	Max Error
		Yakubu&	Yakubu&	First	Second
		Sibanda (2024)	Sibanda (2024)	Derivative	Derivative
20	1	3.36×10^{-03}	2.64×10^{-04}	2.15×10^{-02}	4.90×10^{-05}
40	20 1	1.18×10^{-04}	1.80×10^{-06}	2.81×10^{-03}	3.27×10^{-07}
30	40 1	2.42×10^{-06}	1.87×10^{-08}	1.76×10^{-04}	5.07×10^{-10}
160	80 1	4.10×10^{-08}	1.64×10^{-10}	7.83×10^{-06}	5.98×10^{-13}
320	$\frac{160}{1}$	6.57×10^{-10}	1.34×10^{-12}	2.78×10^{-07}	2.44×10^{-15}

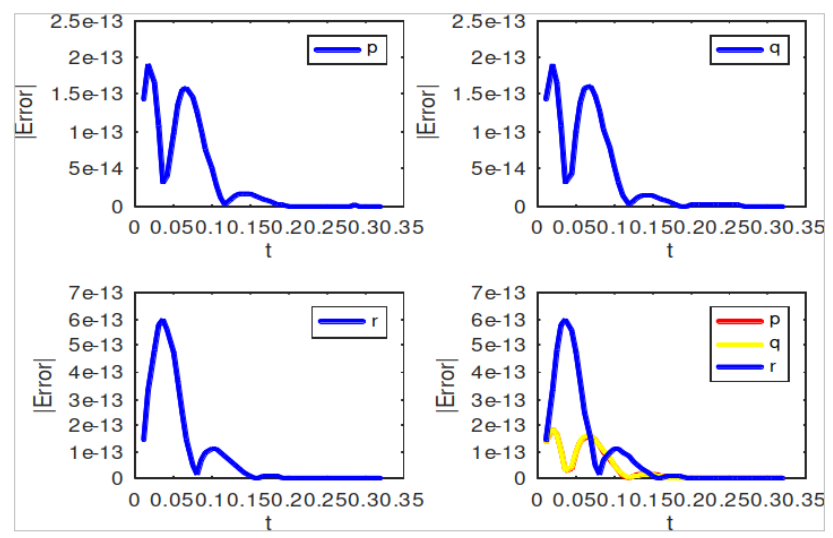


Figure 3: Convergence plot of Example 1 against t using the new second derivative block method

Example 2 Network Problem

Reaction rates are usually called velocities in this parlance. Let v_i , i = 1,2,3,4,5 be the reaction rates in a given network graph. Suppose reaction rates are given by the following mass action:

$$v_1 = k_1, v_2 = k_2[P], v_3 = k_3[P][Q], v_4 = k_4[R], v_5 = k_5[S].$$

Let the concentrations of the corresponding species be p,q,r,s. Given that the rate constants $k_1=3 \text{nM/sec}, k_2=2 \text{nM/sec}, k_3=2.5 \text{nM/sec}, k_4=3 \text{nM/sec}, k_5=4 \text{nM/sec}$, the species concentrations satisfy the following set of differential equations, expressed in nM/sec

$$\frac{d}{dt}(p(t)) = 3 - 2.5p(t)q(t) - 2p(t)$$

$$\frac{d}{dt}(q(t)) = 2p(t) - 2.5p(t)q(t)$$

$$\frac{d}{dt}(r(t)) = 2.5p(t)q(t) - 3r(t)$$

$$\frac{d}{dt}(s(t)) = 2.5p(t)q(t) - 4s(t).$$

All species start with initial concentrations of zero at time t = 0. In this example, we used a constant step size h = 0.01. Computational results are as shown in Figure 4 and Table 4.

Table 4: Results of using both First Derivative and NOSDBHLMM on Example 3 with a Constant Step Size h = 0.01

t	у	New First Derivative Computed Concentrations	New Second Derivative Computed Concentrations
	p(t)	0.862099414	0.862098107
1.0	q(t)	0.660900099	0.660901374
	r(t)	0.350847134	0.350848147
	s(t)	0.290777135	0.290777870
	p(t)	0.767747763	0.767747605
2.0	q(t)	0.781347539	0.781347684
	r(t)	0.491363558	0.491363593
	s(t)	0.372857774	0.372857775
	p(t)	0.752529641	0.752529621
3.0	q(t)	0.797194540	0.797194561
	r(t)	0.499479528	0.499479529
	s(t)	0.374892820	0.374892820
	p(t)	0.750380222	0.750380219
4.0	q(t)	0.799570984	0.799570987
	r(t)	0.499949401	0.499949401
	s(t)	0.374980699	0.374980699

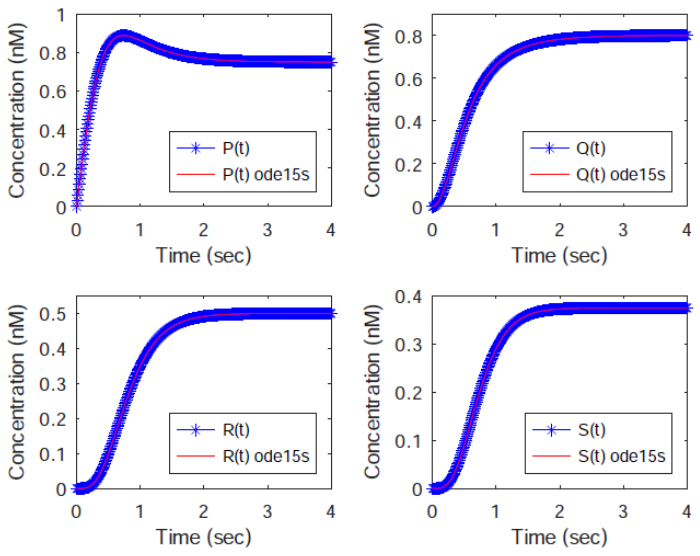


Figure 4: Concentrations of the species P, Q, R, S for $0 \le t \le 4$ and h = 0.01 using the new derivative method

Example 3: HIRES Problem

This problem was introduced by Schaffer in 1975. It stems from the High Irradiance Response (HIRES) of photomorphogenesis on the grounds of phytochrome. The corresponding chemical reaction consists of 8 reactants which leads to the following system of stiff differential equations.

$$\begin{aligned} y_1{}' &= -1.7y_1 + 0.43y_2 + 8.32y_3 + 0.0007 \\ y_2{}' &= 1.7y_1 - 8.75y_2 \\ y_3{}' &= -10.03y_3 + 0.43y_4 + 0.035y_5 \\ y_4{}' &= 8.32y_2 + 1.71y_3 - 1.12y_4 \\ y_5{}' &= -1.745y_5 + 0.43y_6 + 0.43y_7 \\ y_6{}' &= -280y_6y_8 + 0.69y_4 + 1.71y_5 - 0.43y_6 + 0.69y_7 \\ y_7{}' &= 280y_6y_8 - 1.81y_7 \\ y_8{}' &= -280y_6y_8 + 1.81y_7, \end{aligned}$$
 Satisfying the initial conditions $y = [1, 0, 0, 0, 0, 0.0057]$.

Table 5: Solution of the HIRES Problem at t = 5 and t = 350 Minutes using the New FDBHLMM

y_i	Amat et al	FDBHLMM	FDBHLMM	FDBHLMM
	Solution at $t = 5$	Solution at $t = 5$	Solution at $t = 5$	Solution at $t = 5$
		h = 0.1	h = 0.01	h = 0.001
y_1	0.03209606	0.031957132	0.031957517	0.031957522
y_2	0.00657329	0.006505570	0.006505644	0.006505645
y_3	0.00464137	0.004593266	0.004593343	0.004593344
y_4	0.09110392	0.089979580	0.089980189	0.089980195
y_5	-	0.162306779	0.162321575	0.162321737
y_6	-	0.684539117	0.684599106	0.684599764
y_7	0.00572391	0.005646663	0.005646666	0.005646666
y_8	0.00005439	0.000053337	0.000053334	0.000053334
	Solution at $t = 350$		Solution at $t = 350$	
y_5	0.00053631	0.000602815	0.000602855	0.000602856
y_6	0.00115496	0.001416771	0.001416857	0.001416858

Table 6: Solution of the HIRES Problem at t = 5 and t = 350 Minutes using the Second Derivative Block Hybrid Method

y_i	Amat et al	NOSDBHLMM	NOSDBHLMM
	Solution at $t = 5$	Solution at $t = 5$	Solution at $t = 5$
		h = 0.1	h = 0.01
y_1	0.03209606	0.031962018	0.031957518
y_2	0.00657329	0.006506512	0.006505644
y_3	0.00464137	0.004594251	0.004593343
y_4	0.09110392	0.089987280	0.089980189
y_5	-	0.162495583	0.162321591
y_6	-	0.685304538	0.684599169
y_7	0.00572391	0.005646722	0.005646666
y_8	0.00005439	0.000053278	0.000053334
	Solution at $t = 350$	Solution at $t = 350$	
y_5	0.00053631	0.000603326	0.000602855
y_6	0.00115496	0.001417876	0.001416858

Table 6 summarizes the results of the HIRES problem at specific times (5 and 350 minutes), offering a comparative look at the performance of different numerical methods over time.

Table 7: Absolute error of the HIRES problem at t = 5 and t = 350 minutes using the new FDBHLMM

- Yi	Amat et al (2019)	FDBHLMM	FDBHLMM	FDBHLMM
	Error at $t=5$	Error at $t=5$	Error at $t=5$	Error at $t=5$
		h = 0.1	h = 0.01	h = 0.001
y 1	1.64×10^{-04}	2.54×10^{-05}	2.58×10^{-05}	2.58×10^{-05}
y 2	7.28×10^{-05}	5.08×10^{-06}	5.15×10^{-06}	5.16×10^{-06}
y ₃	5.21×10^{-05}	3.95×10^{-06}	4.03×10^{-06}	4.03×10^{-06}
y 4	1.21×10^{-03}	9.05×10^{-05}	9.11×10^{-05}	9.12×10^{-05}
y 5	-	4.87×10^{-05}	3.39×10^{-05}	3.37×10^{-05}
y 6	-	1.52×10^{-04}	9.29×10^{-05}	9.22×10^{-05}
y 7	7.73×10^{-05}	4.04×10^{-09}	7.04×10^{-09}	7.04×10^{-09}
y 8	1.05×10^{-06}	4.04×10^{-09}	7.04×10^{-09}	7.04×10^{-09}
-	Error at $t = 350$		Error at $t = 350$	
y 5	6.67×10^{-05}	1.65×10^{-07}	1.25×10^{-07}	1.24×10^{-07}
У6	2.62×10^{-04}	4.07×10^{-07}	3.21×10^{-07}	3.20×10^{-07}

Table 8: Absolute error pf the HIRES problem at t = 5 and t = 350 minutes using the second derivative block hybrid method

y i	Amat et al (2019) Error at <i>t</i> = 5	NOSDBHLMM Error at t = 5 h = 0.1	NOSDBHLMM Error at <i>t</i> = 5 <i>h</i> = 0.01
y ₁	1.64×10^{-04}	$\frac{n-0.1}{3.03\times 10^{-05}}$	$\frac{n - 0.01}{2.58 \times 10^{-05}}$
y ₂	7.28×10^{-05}	6.02×10^{-06}	5.15×10^{-06}
y3	5.21×10^{-05}	4.94×10^{-06}	4.03×10^{-06}
y4	1.21×10^{-03}	9.82×10^{-05}	9.11×10^{-05}
y 5	-	1.40×10^{-04}	3.39×10^{-05}
У6	-	6.13×10^{-04}	9.28×10^{-05}
y 7	7.73×10^{-05}	6.30×10^{-08}	7.04×10^{-09}
y ₈	1.05×10^{-06}	6.30×10^{-08}	7.04×10^{-09}
	Error at $t = 350$	Error at $t = 350$	
y 5	6.67×10^{-05}	3.46×10^{-07}	1.25×10^{-07}
y 6	2.62×10^{-04}	6.98×10^{-07}	3.20×10^{-07}

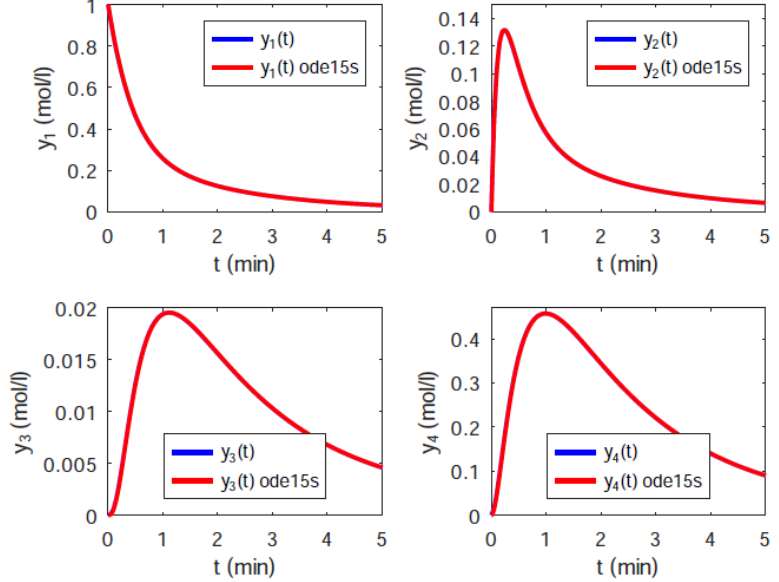


Figure 5: Solution of the HIRES problem at t = 5 min for y_1 , y_2 , y_3 , y_4

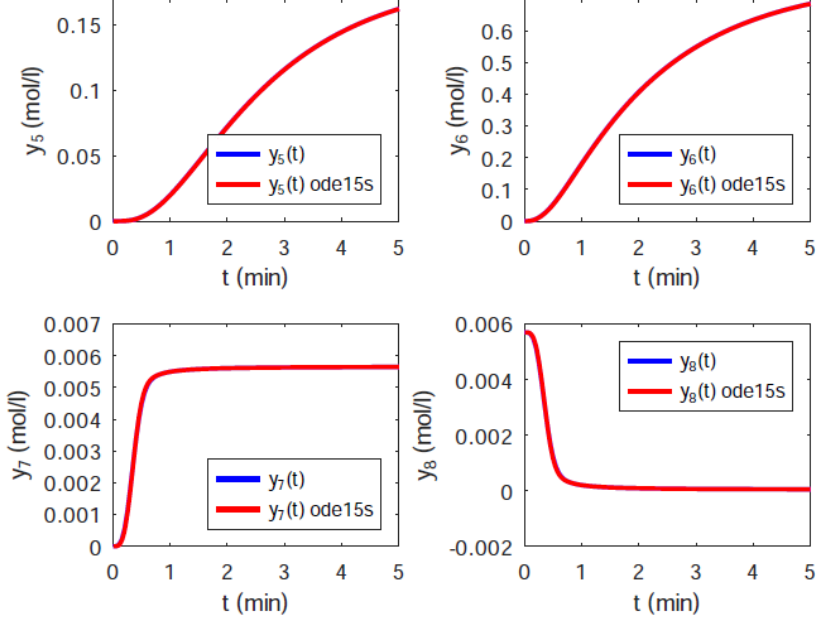


Figure 6: Solution of the HIRES problem at t = 5 min for y_5 , y_6 , y_7 , y_8

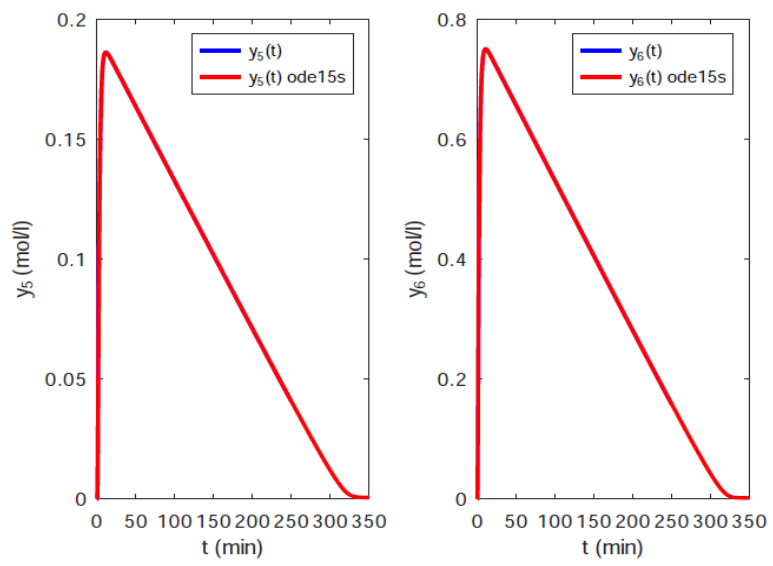


Figure 7: Solution of the HIRES problem at t = 350 min for y_5 , y_6

Discussion of Results

In this paper, we presented two block hybrid methods with non-equidistant grid points. The FDHBLMM is a fifth–order first derivative block hybrid method with a small region of absolute stability, while the second method NOSDBHLMM is of ninth–order with a large region of absolute stability. Both methods are A(a)–stable, zero-stable, consistent and convergent. In actual fact, the NOSDBHLMM is an extension of the FDHBLMM; which gives better approximations to the exact solution though it involves more function evaluations. However, the FDHBLMM is faster because it has less function evaluations per block suffers the 'disadvantage' of not being as accurate as the NOSDBHLMM. The better accuracy of NOSDBHLMM is due to its larger region of absolute stability as well as smaller error constant than the FDHBLMM.

Figure 3 shows the convergence plots for Example 3.1 against time. These plots demonstrate how the numerical solutions approach the exact solution over time. Besides this, column six of Table 3 shows that the new NOSDBHLMM had the smallest maximum absolute error when compared to the two methods of Yakubu and Sibanda (2024). This confirms the accuracy of our new method for the solution of first order linear IVPs. Table 4 and Figure 4 shows the table and figures after applying the new methods in solving the Network problem in Example 3.2. The solution of our methods coincide to a greater extent with those of ode15s.

Figures 5 to 7 present the results of the HIRES problem at different times (5 minutes and 350 minutes) for different species with varying step sizes (h = 0.1, 0.01, 0.001). These figures are crucial in comparing how different step sizes affect the numerical solution of the HIRES problem in comparison to those of Amat et al (2019) and ode15s. Figure 5 shows the trajectory of the solution of our new NOSDBHLMM when superimposed with those of ode15s for y1, y2, y3, y4 while Figure 6 depicts those for y4, y5, y6, y7 at time t = 5 minutes. Furthermore, we did the same thing at time t = 350 minutes for y5 and y6 in accordance with Amat et al., (2019), albeit Amat et al (2019) did not compare their solution with the well known stiff solver ode15s.

In Tables 5 and 6, we present the solution of the HIRES problem at t = 5 and t = 350 minutes

Using Amat et al. (2019) variational method, new FDHBLMM and NOSDBHLMM methods respectively. The dash in all the tables signifies that the values were not

available in the literature. Table 7 shows a comparison of the absolute error of the HIRES problem at t = 5 and

t=350 minutes using Amat et al., (2019) and the new FDBHLMM for h=0.1, h=0.01, h=0.001. The table showed that the new method outperformed those in [16]. Similar results can be seen in Table 8 for h=0.1 and h=0.01. Due to the computational time involved, for h=0.001 we could not compute the solution using the NOSDBHLMM. As stated earlier, for the purpose of our comparison, we used the solution provided by ode15s as the exact. The good performance of our method when compared to the variational method in Amat et al., (2019) shows that our method is reliable and can be applied in solving both linear and nonlinear IVPs.

CONCLUSION

This article successfully developed and analyzed first and second-order methods for solving the

HIRES problem in photovoltaic cells. By focusing on the stability and convergence of these methods, it was demonstrated that the proposed algorithms provide significant improvements over traditional numerical methods. The first-order method adapted to fluctuating irradiance levels, enhancing stability and reducing computational cost. Moreso, the second-order method improved accuracy and stability that makes it suitable for long-term simulations. The results indicate that the new methods are robust and capable of handling the challenges associated with high irradiance conditions. The convergence plots and stability analysis confirm that these methods are reliable for practical applications. The numerical experiments showed that the proposed methods outperform existing techniques, providing more accurate and stable solutions.

REFERENCES

Abdullahi H. (2018). Development of block unification hybrid linear multistep methods forfluid flow equations (Doctoral dissertation, Federal University of Technology, Minna).

Akinola R. O. and Akoh A. S. A Seventh-order computational algorithm for the solution of stiff systems of differential equations. Journal of the Nigerian Mathematical Society. Vol. 42, Issue 3, pp. 215 - 242, 2023.

Amat S, Maria Jose Legaz M. J. & Ruiz-Alvarez J(2019). On a Variational Method for Stiff Differential Equations Arising from Chemistry Kinetics. MDPI Mathematics, 7(5), 45–49; https://doi.org/10.3390/math7050459

Bennett J. C., Krishnamoorthy V., Liu S., Grout R. W., Hawkes E. R., & Chen J. H. (2011). Feature-based statistical analysis of combustion simulation data. IEEE Transactions on Visualization and Computer Graphics, 17(12), 1822–1831.

Castro R., Bergonzi M., & Kofman E. (2024). Discrete-event simulation of continuous-time systems: Evolution and state of the art of quantized state system methods. Simulation, 100(6).

Hawagfeh N. S., & Kaya D. (2004). Comparing numerical methods for the solutions of systems of ordinary differential equations. Applied Mathematics Letters, 17(3), 323–328.

Henrici P., Discrete variable methods in ODE. New York, USA: John Wiley & Sons, 1962.

Jacobson, M. Z. (2005). Fundamentals of atmospheric modeling (2nd ed.). Cambridge University Press.

Kowalski K., Bair R., Bauman N. P., Boschen J. S., Bylaska E. J., Daily J., de JongW. A., Dunning Jr. T., Govind N., Harrison R. J., Keceli M., Keipert K., Krishnamoorthy S., Kumar S., Mutlu E., Palmer B., Panyala A., Peng B., Richard R. M., Straatsma T. P., Sushko P., Valeev E. F., Valiev M., van Dam H. J. J., Waldrop J. M., Williams-Young D. B., Yang C., Zalewski M., & Windus Lambert, J. D. Computational Methods in Ordinary Differential Equations; John Wiley: New York, NY, USA, 1973.

Lu T., & Law C. K. (2009). Toward accommodating realistic fuel chemistry in large-scale computations. Progress in Energy and Combustion Science, 35(2), 192–215.

Mashruk S., Shi H., Mazzotta L., Ustun C. E., Aravind B., Meloni R., Alnasif A., Boulet E., Jankowski R., Yu C., Alnajideen M., Paykani A., Maas U., Slefarski R., Borello D., & Valera- Medina A. (2024). Perspectives on NOx emissions and impacts from ammonia combustionprocesses. Energy & Fuels, 38(15), 19253–19292.

Okuonghae R. I. and Ikhile M. N. O., Continuous formulation of $A(\alpha)$ -Stable Second derivative linear multistep methods for Stiff initial value problems in ordinary differential equations. Journal of Algorithms and Computational Technology, 6, 175–190.

Onumanyi, P., Awoyemi, D. O., Jator, S. N. and Sirisena, U. W. (1994) New Linear Multistep Methods with Continuous Coefficients for First Order Initial Value Problems. Journal of Nigeria Mathematics Society, 13, 37-51.

Rufai M. A. (2024). Numerical integration of third-order BVPs using a fourth-order hybrid block method. Journal of Computational Science, 81, 102338.

Simon H. D., Zacharia T. & Stevens R. L. (2007). Modeling and simulation at the exascale for energy and the environment. Lawrence Berkeley National Laboratory.

Singh G., Garg A., Singla R., & Kanwar V. (2021). A novel two-parameter class of optimize hybrid block methods for integrating differential systems numerically. Computational and Mathematical Methods, 3(6), e1214.

Smith, J., & Anderson, P. (2005). A First-Order Approach to High Irradiance Problems." Journal of Photovoltaic Research, 12(3), 215–225.

Spiteri R. J. (1997). Solution methods for differential systems subject to algebraic inequality constraints (T). University of British Columbia. Retrieved from https://open.library.ubc.ca/collections/ubctheses/831/items/1.0080007

T. L. (2021). From NWChem to NWChemEx: Evolving with the computational chemistry landscape. Chemical Reviews, 121(10), 4962–4998.

Trieschmann J., Vialetto L., & Gergs T. (2023). Machine learning for advancing lowtemperature plasma modeling and simulation. Journal of Micro/Nanopatterning, Materials, and Metrology, 22(4), 041504.

Yakubu S. D. and Sibanda P. (2024) One–Step Family of Three Optimized Second–Derivative Hybrid Block Methods for Solving First–Order Stiff Problems. Hindawi Journal of Applied Mathematics Volume 2024, Article ID 5078943, https://doi.org/10.1155/2024/5078943

Zhang T., Yi Y., Xu Y., Chen Z. X., Zhang Y., & Xu, Z.-Q. J. (2022). A multi-scale sampling method for accurate and robust deep neural network to predict combustion chemical kinetics. Combustion and Flame 245 (2022) 112319.



©2025 This is an Open Access article distributed under the terms of the Creative Commons Attribution 4.0 International license viewed via https://creativecommons.org/licenses/by/4.0/ which permits unrestricted use, distribution, and reproduction in any medium, provided the original work is cited appropriately.